Interaction of Small Peptides with Lipid Bilayers

K. V. Damodaran,* Kenneth M. Merz, Jr.,* and Bruce Paul Gaber‡
*Department of Chemistry, The Pennsylvania State University, University Park, Pennsylvania 16802; and ‡Center of Bio/Molecular Science and Engineering, Naval Research Laboratory, Washington, DC 20375

ABSTRACT Molecular dynamics simulations of the tripeptide Ala-Phe-Ala-O-tert-butyl interacting with dimyristoylphosphatidylcholine lipid bilayers have been carried out. The lipid and aqueous environments of the peptide, the alkyl chain order, and the lipid and peptide dynamics have been investigated with use of density profiles, radial distribution functions, alkyl chain order parameter profiles, and time correlation functions. It appears that the alkyl chain region accommodates the peptides in the bilayer with minimal perturbation to this region. The peptide dynamics in the bilayer bound form has been compared with that of the free peptide in water. The peptide structure does not vary on the simulation time scale (of the order of hundreds of picoseconds) compared with the solution structure in which a random structure is observed.

INTRODUCTION

The molecular level details of how membrane structure, function, and dynamics are affected by intercalated molecules is poorly understood, but is critical in increasing our understanding of how biomembranes mediate processes between the interior of a cell and its surrounding environment (Gennis, 1989). Recently, many studies have examined the thermodynamic and structural aspects of the partitioning of various guests into model membranes. The desolvation of the guests and the structural perturbation induced in the bilayer as a result of the intercalation process play a crucial role in determining its energetics. Seelig and co-workers have investigated a number of small molecules and peptides by using calorimetric methods (Seelig and Ganz, 1991; Beschiaschvili and Seelig, 1992). These molecules partition into the bilayer by the "nonclassical hydrophobic effect," which is an enthalpy-driven process ($\Delta S_{tran} \sim 0$) and not an entropic one like the classical hydrophobic effect (Tanford, 1980). Seelig and Ganz (1991) have suggested that in the case of amphiphilic molecules partitioning into membranes, the nearly zero entropy of transfer is attributable to compensating contributions from the desolvation of the amphiphile and the increased hydration of the bilayer interface during the insertion. Hence, the apparent free energy of transfer is mostly made up of the enthalpic part due to the van der Waals interaction between the amphiphile and the hydrophobic core of the bilayer.

Not all molecules that intercalate into a lipid bilayer show the thermodynamic properties associated with the nonclassical hydrophobic effect. For example, Jacobs and White (1986, 1987, 1989) used various techniques to investigate a series of tripeptides (Ala-X-Ala-O-tert-butyl with X = Trp, Phe, Leu, Ala, Gly) interacting with phosphatidylcholine-based bilayers. The temperature dependence of the binding constants suggests that the peptide partitioning into the liquid crystalline bilayer phase is entropy-driven (the classical hydrophobic effect), with the observed enthalpy of transfer being zero. These peptides were synthesized such that the hydrophobic tert-butyl end would enhance the insertion of the peptide into the hydrocarbon interior of the bilayer, and the amino terminus would anchor itself at the aqueous interface (Jacobs and White, 1986). Neutron diffraction studies of the peptide on oriented dioleoylphosphatidylcholine (DOPC) bilayers suggested that the peptide was predominantly confined to the interfacial region with the central residue (X) exposed to the hydrocarbon region (Jacobs and White, 1989). Recent nuclear magnetic resonance (NMR) investigations (Brown and Huestis, 1993) using nuclear Overhauser enhancements (NOE) of Ala-Phe-Ala-O-tert-butyl (AFAtBu) bound to dimyristoylphosphatidylcholine (DMPC) and DOPC vesicles have given more insights into the conformation and orientation of these peptides in the membrane bound state. They have shown that the tert-butyl group of the peptides has significant interaction with the alkyl chain region, whereas the central residue is located near the lipid ester region. Furthermore, these studies show that the peptide adopts a "preferred conformation," as opposed to the random structure in solution.

In order to garner a molecular level understanding of how these peptides interact with biomembranes, we have investigated these systems by using molecular dynamics (MD) simulations. The availability of detailed structural and thermodynamic data makes this system particularly attractive for simulation studies. Furthermore, the size of these peptides allows them to be simulated with a relatively small number of lipids. Herein we describe an analysis of the structural and dynamical perturbations induced in a DMPC bilayer by the intercalated AFAtBu peptides.

Received for publication 20 October 1994 and in final form 10 July 1995.
Address reprint requests to Dr. Kenneth M. Merz, Jr., Department of Chemistry, Pennsylvania State University, 153 Davey Laboratory, University Park, PA 16802-2801. Tel.: 814-865-3623; Fax: 814-863-8403; E-mail: merz@retina.chem.psu.edu.

0006-3495/95/10/1299/10 $2.00

MATERIALS AND METHODS

The model

The initial structure for the MD simulation was built by placing 32 DMPC lipids to form two leaflets (16 × 2), with the head groups facing each other, with a surface area of 66 Å^2/lipid (Lewis and Engelman, 1983). The lipids were randomly oriented in the plane of the leaflets, with particular care taken to avoid any bad van der Waals contacts. Our earlier simulations of neat DMPC bilayers with initial structures built using this scheme have shown that the randomly oriented starting structure would avoid the "collective tilt" of the alkyl chains observed when the starting structure was built from the crystal structure in which the alkyl chains are parallel to one another (Damodaran and Merz, 1994). This scheme also gives molecular order parameter profiles that are in better agreement with experimental results.

Two models were simulated with the peptides bound in different orientations. Earlier neutron diffraction data (Jacobs and White, 1989) suggested that the peptide backbone might be parallel to the bilayer surface with the central residue (Trp in their experiments) exposed to the hydrophobic region. However, the orientation of the peptide based on NOE data (Brown and Heustis, 1993), has suggested that the tert-butyl group is inserted into the hydrophobic region. We have investigated two models built according to these results. In the model with the peptide backbone parallel to the bilayer surface (model I), the tert-butyl group was more exposed to water throughout simulation. In the second model (model II), the starting structure of the peptide was generated by restraint minimization consistent with the NOEs observed by Brown and Huestis (1993). Furthermore, care was taken during the placement of the peptides to have the tert-butyl groups below the lipid head groups, as observed in the NMR study (Brown and Huestis, 1993). Two peptides (AFAtBu) were docked into the bilayer using the computer graphics program MIDASPlus (University of California San Francisco, CA). Care was taken to avoid any bad nonbond contacts between the peptide and neighboring lipids that might give rise to very large repulsive forces during minimization/MD-equilibration. The bilayer-peptide system was solvated by adding ~25 SPC/E water molecules (Berendsen et al., 1987) per lipid in the interlamellar region. The peptides have an effective charge of +1. Two chloride ions were placed in the aqueous region to render the total system neutral. The starting geometry of the peptides and their lipid neighbors in model II is shown in Fig. 1.

Force field

The partial charges for the lipid and the peptide molecules were obtained with quantum mechanical electrostatic potential fitting on the molecules by using the STO-3G* basis set (Besler et al., 1990; Merz, 1992). The charges used for the peptide are given in Table 1, as is the numbering system that will be used throughout. The partial charges for DMPC molecules has been reported previously (Damodaran and Merz, 1994). Bond, angle, and dihedral parameters were taken from the AMBER force field (Weiner et al., 1984). The van der Waals interactions were modeled with use of the OPLS parameter set with the 1–4 electrostatic and van der Waals interactions scaled by 2 and 8, respectively (Jorgensen and Tirado-Rives, 1988).

MD simulations

MD simulations were carried out by using the parallelized versions (Vincent and Merz, 1995) of the MINMD module from AMBER 4.0 (Pearlman et al., 1991) and the SANDER module from AMBER 4.1 running on the IBM SP1 at The Pennsylvania State University Center for Academic Computing and the CRAY-T3D at the Pittsburgh Supercomputing Center, respectively. The system was held at 315 K, well above the gel-to-liquid crystalline phase transition temperature, by using separate temperature coupling for the bilayer and the solvent (Berendsen et al., 1984). Constant-volume periodic-boundary conditions with a residue-based cut-off distance of 13.5 Å for the nonbonded interactions and a time step of 0.0015 ps were used. The peptide/bilayer models described above were equilibrated by raising the temperature in several stages (0–100 K for 9 ps, 100–200 K for 9 ps, 200–315 K for 9 ps) to the final value of 315 K. At this stage a full equilibration run was performed for 90 ps. Atomic coordinates and velocities were collected every 20 steps (0.030 ps) for 360 ps at 315 K using under constant-volume periodic-boundary conditions. The analyses of the trajectories were carried out by calculating various distribution functions and time correlation functions described below. A trajectory of the peptide solvated in a box of 842 SPC/E water molecules was also collected for 250 ps so that the peptide structure in the bilayer and water could be compared.

RESULTS AND DISCUSSION

Peptide conformation and location

Fig. 2 shows the peptides and their lipid neighbors at the end of the MD trajectory of model II. The Phe-2 side chain and

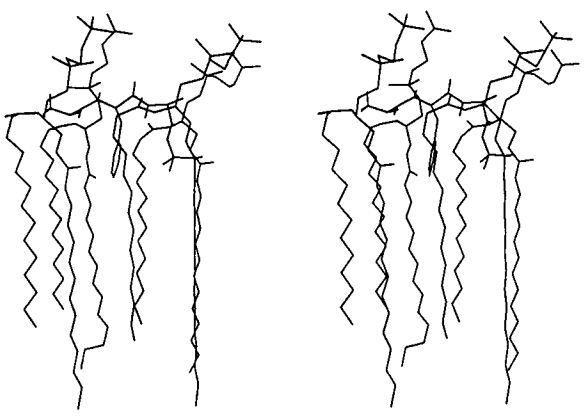

FIGURE 1 The starting geometry of the peptide/lipid system in model II. The peptide geometry was minimized by using the NOE restraints before docking with the bilayer leaflet.

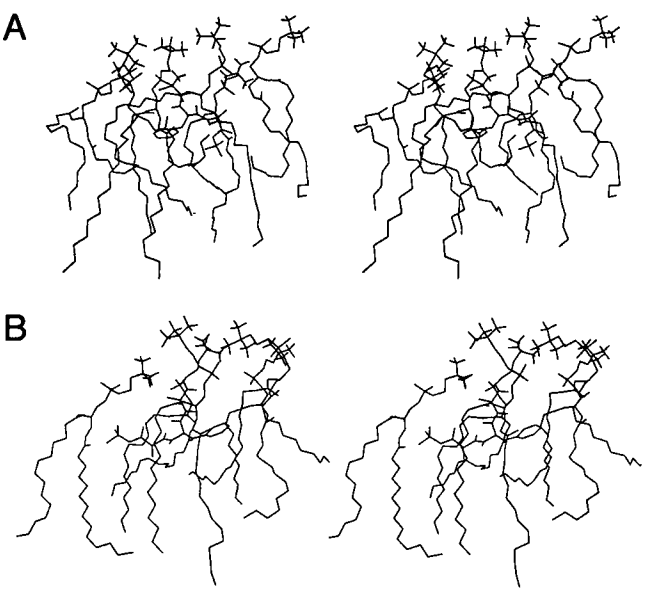

FIGURE 2 Geometry of peptide-1 and peptide-2 and their lipid neighbors after 450 ps of MD simulation (model II).

the tert-butyl group have intercalated between the lipids and maintain van der Waals contacts with the alkyl chains, whereas the N-termini are located near the lipid phosphate groups. In model I however, only the Phe side chains were inserted into the alkyl region, and the peptide backbone remained parallel to the bilayer surface, with the tert-butyl groups located in the same region as the trimethylammonium groups of the lipids. This resulted in a reduction of the conformational flexibility for the peptides, as evidenced in the Ramachandran plots discussed below.

The conformation of the peptide exhibits some degree of randomness in both the solution and the bilayer. This is shown with use of Ramachandran plots in Fig. 3. The observed spread along the ψ-axis for Ala-3 can be related to the mobility of the tert-butyl group at the C-termini, since the linking oxygen was included in the calculation of the angle. In the ϕ-ψ map for the solution run, the points in the $\psi = 100$–$160°$ range for Ala-3 were attributable to a 30-ps long-lived conformation. In addition to this, random fluctuations were also observed in the sterically disallowed regions. ϕ-ψ maps are given for the two peptides together from the bilayer runs. The peptides in model I were limited to β-sheet conformations because of the lack of conformational flexibility mentioned above. In model II, however, the peptides showed greater conformational flexibility, and the similar behavior for Ala-3 as seen in the solution runs was observed. Furthermore, the Phe-2 of the two peptides remained in different regions. Although Phe-2 was in the β-sheet conformation in peptide-1, in peptide-2 it was α-helical.

The average position of the peptides, lipids, and solvent regions of the bilayer using the density profiles along the bilayer normal are shown in Fig. 4. In the following discussion we will focus on model II because it corresponds to the best-characterized positioning for the peptides in a DMPC bilayer (Brown and Huestis, 1993). We also note that many of the properties described below (e.g., probability profiles and lipid dynamics) for model II also hold for model I. The peptide distribution (*shaded regions*) extends from the head group-water interface into the alkyl chain distributions. Although not shown separately, the tert-butyl groups are buried deeper than the Phe side chains (*dark shaded region*) in the alkyl region, as evidenced by the intensity of the total peptide density profile. The position of the peptide density profile with respect to the lipid distributions agrees with neutron diffraction results (Jacobs and White, 1989). Furthermore, the orientation of the peptides is consistent with the NMR results (Brown and Huestis, 1993) with respect to the positions of the Phe side chain and the tert-butyl group. The counter ions included in the simulation have a rather wide distribution, indicating that they do not have any site preference. Other features of the probability distributions in Fig. 4 are similar to our earlier simulation of neat DMPC bilayers and will not be discussed further (Damodaran and Merz, 1994).

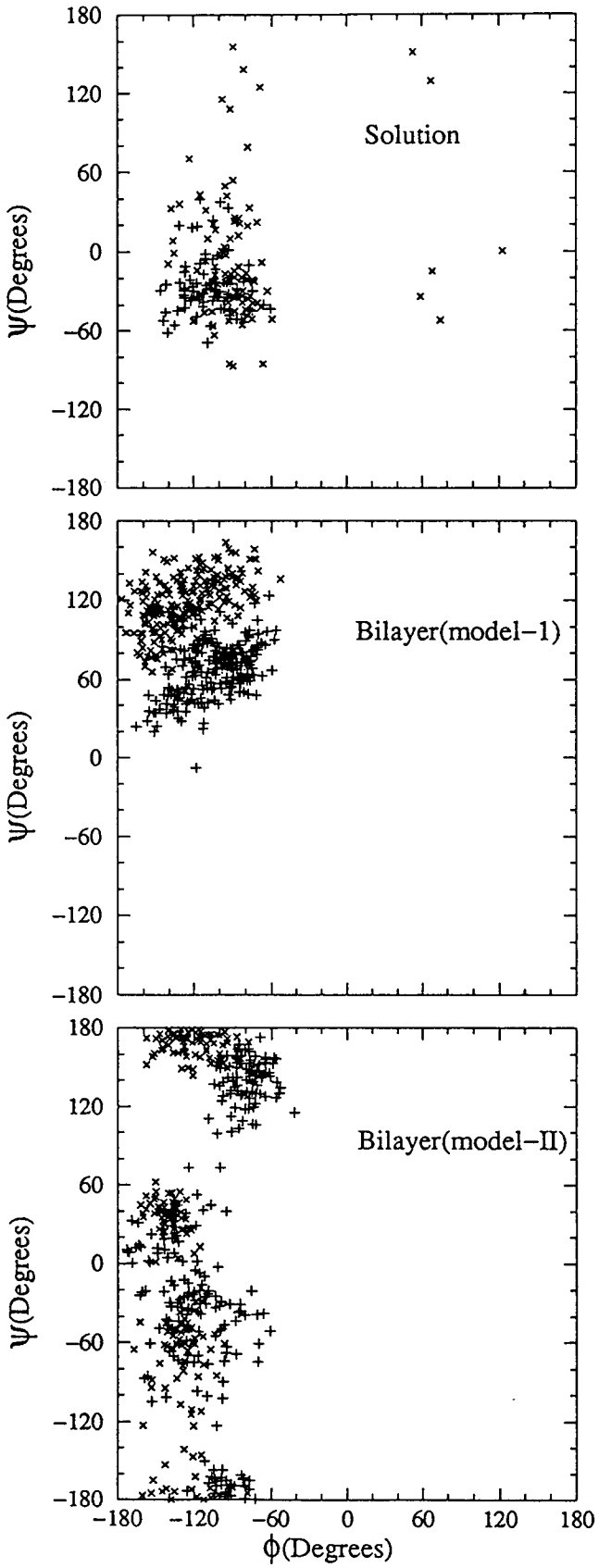

FIGURE 3 Ramachandran plots for Phe-2 (+) and Ala-3 (x). The data were collected every 3 ps along the trajectory. In the bilayer bound form, the figures include data from both peptide-1 and peptide-2.

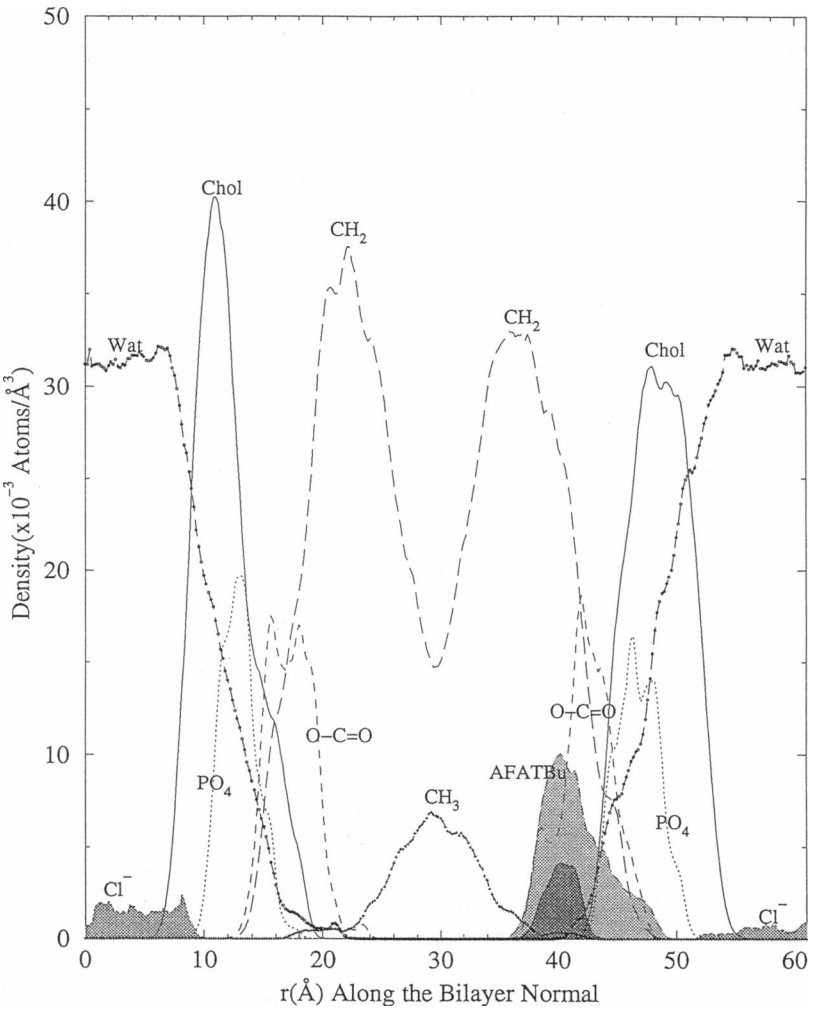

FIGURE 4 Density profiles for the peptides, different lipid regions, and water along the bilayer normal. The peptide distribution is shaded with the Phe-2 side chains shown in darker shade. The counter ion density values have been multiplied by 10 to have visible intensities. This profile is for model II only, but model I gives qualitatively similar results. Chol, choline head group; CH_2, methylene carbons of the alkyl chains; CH_3, terminal methyl group of the alkyl chains; O—C═O, carbonyl groups of the lipids; PO_4, lipid phosphate group; Cl^-, chloride counter ions; Wat, water.

Radial distribution functions

We have probed the water and lipid environments of the peptide by using pair distribution functions ($g(r)$) for water and histograms for lipids. The pair distribution functions were calculated as:

$$g(r) = N(r)/4\pi r^2\rho_0 \quad (1)$$

where $N(r)$ is the number of water molecules between r and $r + dr$, and ρ_0 is number density of water. Lipid environments of the peptide have been represented as histograms ($N(r)$ in Eq. 1.

The peptide N-termini are located near the head group water interface and not unexpectedly have clear hydration shells, as seen from the pair distribution functions of water oxygens in Fig. 5 *a*. They also have close interactions with the nonesterified oxygens of the phosphate groups, as shown by the histograms in Fig. 5 *b*. When the oxygen coordination numbers at an arbitrary cut-off distance of 4 Å are considered, peptide-1 has a slightly higher oxygen coordination number than does peptide-2 (5.9 vs. 5.1). The lipid choline head groups have rather similar distribution around the peptide N-termini, as seen in Fig. 5 *c*. The microenvironments of the peptides can differ, depending of the orientation and location of the peptides, because of the highly inhomogeneous nature of the bilayer-solvent interface.

The microenvironments of interest for the tert-butyl groups and the Phe side chains are shown in Fig. 6. These groups are buried in the alkyl chain region and have very few water molecules around them, as shown by the $g(r)$ plots for the tert-butyl groups and the centroid of the Phe side chains in Fig. 6, *a* and *b*, respectively. At an arbitrary 5.0 Å cut-off, peptide-1 has 0.1 water molecules whereas peptide-2 has ~2 (1.6) water molecules around the tert-butyl groups, suggesting that the tert-butyl group of peptide-1 is more deeply buried. This is confirmed further by the distribution of water around the Phe side chains shown in Fig. 6 *b*, where the onset distance of $g(r)$ for peptide-1 is >3.5 Å farther out than that for peptide-2.

The main hydrophobic interactions between the peptide and the bilayer are between the Phe side chain and the tert-butyl group of the peptide and the alkyl chain carbons of the bilayer lipids. The histograms corresponding to these interactions are shown in Fig. 6, *c* and *d*. These histograms

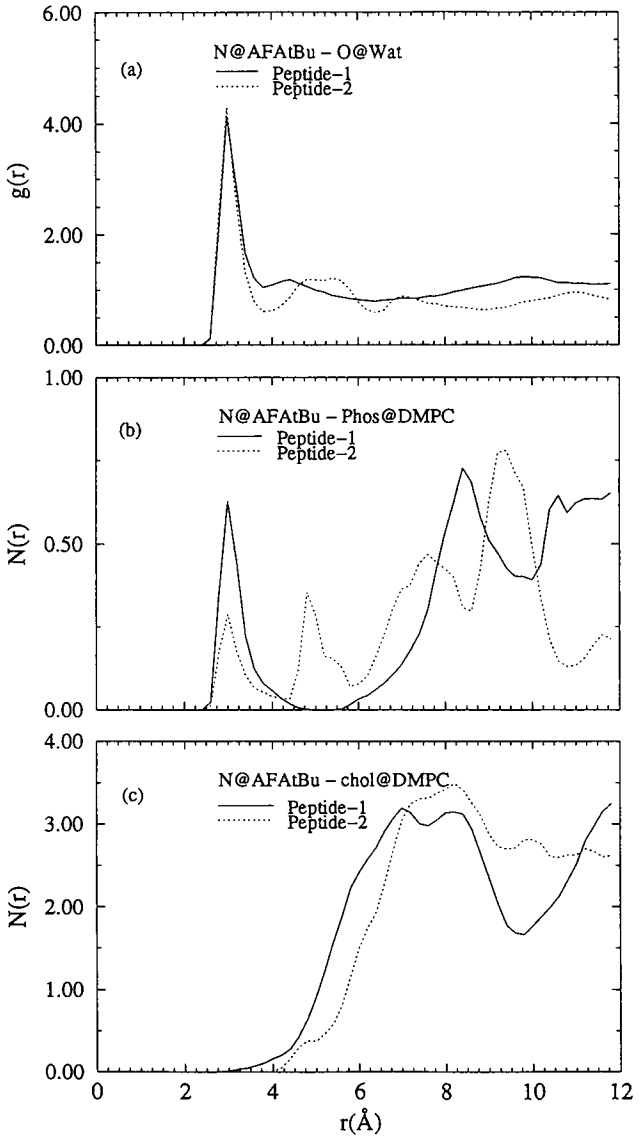

FIGURE 5 (*a*) Water oxygen pair distribution functions and histograms for (*b*) the nonesterified oxygens of the lipid phosphate groups and (*c*) the choline head groups from the peptide amino termini. Data are for model II only.

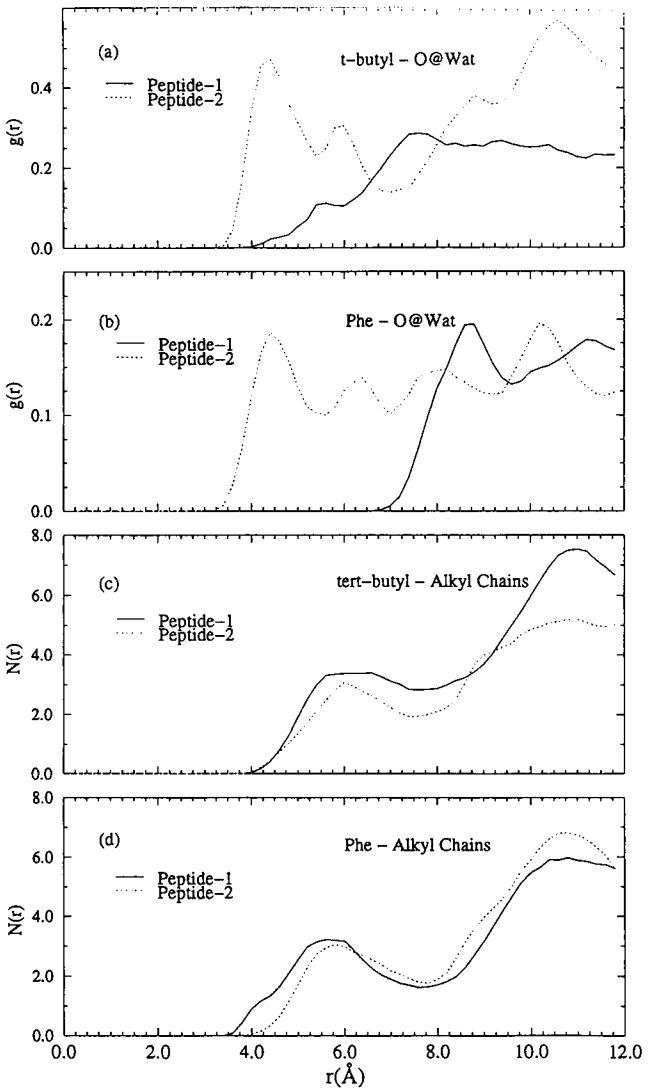

FIGURE 6 Water pair distribution functions from peptide t-butyl groups (*a*) and the centroid of the Phe-2 side chains (*b*), and histograms for the alkyl chains distribution from the tert-butyl groups (*c*) and the centroid of the Phe-2 side chains (*d*). Data are for model II only.

are similar for both peptides and have a clear first-neighbor peak. The flexible nature of the alkyl chains allow even the terminal methyl carbons to have close contacts with these peptide groups and indeed to contribute to the first peak.

The environments of the two peptides presented here show overall similarities. The differences observed in the histogram/pair distribution function plots can be related to the inhomogeneous nature of the lipid-water interface, to the low mobility of the interface region, and to slight differences in the location of the peptide with respect to the neighboring lipids, which are all interrelated. For example, the distribution of water becomes highly inhomogeneous in the vicinity of the lipid phosphate and carbonyl groups, which coupled with slightly different extents of penetration of the Phe side chains into the alkyl chain region, contributes to very different $g(r)$ plots in Fig. 6 *b*. Also note that the intensity on the ordinate itself is very small. It may be possible to eliminate these differences by performing a large number of simulations with different starting configurations for relatively shorter time scales and by averaging the environments over the individual trajectories. Even with such averaging the contributions caused by the inherent inhomogeneity of the interface would remain. In the absence of such data, it is more appropriate to present the environments of each peptide independently.

Bilayer perturbations

Order parameter profiles

The calculated order parameter profiles of the two leaflets in the system are shown in Fig. 7 *a* for model I and *b* for model

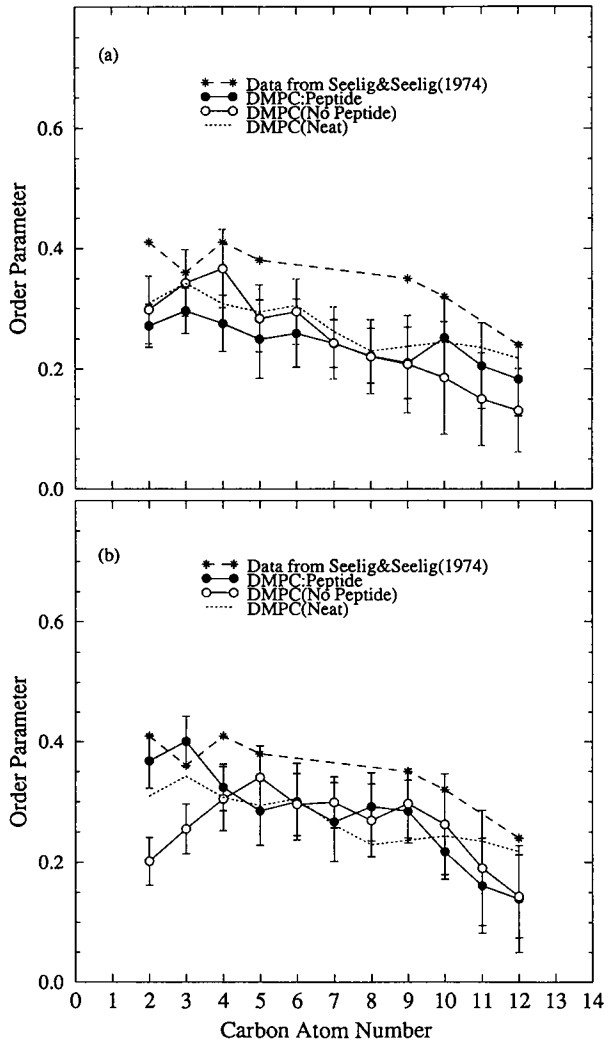

FIGURE 7 Order parameter profiles for the peptide-lipid system from model I (*a*) and model II (*b*).

II. The profile from a neat DMPC simulation (Damodaran and Merz, 1994) and the experimental profile for dipalmitoylphosphatidylcholine by Seelig and Seelig (1974) are also included in these figures for comparison. The experimental profile is at a lower reduced temperature (Seelig and Browning, 1978) ($T_r = 0.5$; $T_r = (T\text{-}T_c)/T_c$, where T_c is the gel-liquid crystalline phase transition temperature and T is the simulation temperature) than both neat DMPC ($T_r = 0.60$) and peptide/DMPC simulations ($T_r = 0.67$) (Jacobs and White, 1986). Hence the experimental order parameters are higher than the calculated values. We have also shown the root-mean-square (RMS) deviations calculated by using Eq. 2 as error bars for the leaflets with and without peptides.

$$(RMS)_i = \left\{ \frac{1}{N_L N_F} \sum_{L}^{N_L} \sum_{F}^{N_F} (S_{iL} - \langle S_{iL} \rangle)^2 \right\}^{1/2} \qquad (2)$$

Where S_{iL} is the instantaneous value of the order parameter, $\langle S_{iL} \rangle$ is the average order parameter for a given carbon atom. N_L is the number of lipids and N_F is the number of coordinate frames considered in the averaging. The perturbation of the alkyl chains is limited to the carbonyl region. In model I (Fig. 7 *a*), where only the central Phe side chains had significant van der Waals contacts with the alkyl chains, a decrease in the order parameters for carbons 2–6 was observed. However, in model II, where the peptides were observed to be more deeply buried, increased order parameters were observed for carbons 2 and 3, whereas the order parameters for the rest of the chain did not show any clear differences. Particularly, in both simulations, the order parameters for the perturbed and unperturbed leaflets are all within the calculated standard deviations from the neat DMPC values. This behavior is similar to the response observed in the presence of small solutes such as benzene, which undergo nearly isotropic motion without severely perturbing the alkyl chain order, particularly at the bilayer center (Bassolino-Klimas et al., 1993). There is an overall increase in the RMS deviations in Fig. 9 from the carbonyl end to the methyl end of the alkyl chains. This might be expected because the methyl end is more mobile, and the finite length of the simulations do not thoroughly average the order parameters, whereas the RMS deviations are relatively lower at the less mobile carbonyl end.

The NMR measurements on DMPC bilayers with different Ala-X-Ala-O-tert-butyl tripeptides showed that the peptide introduced more disorder in the alkyl chains (Jacobs and White, 1987). The perturbation was more pronounced for large hydrophobic side chains, such as Trp and Phe, compared with smaller side chains (Ala). This effect is not clearly borne out in our simulations. As we indicate below, the peptides have not caused significant perturbation on the short-time lipid dynamics. We believe that this is attributable to the lower peptide/lipid ratio (1:8) used in the simulation, compared with that used in the NMR study (1:5) (Jacobs and White, 1987), or to a 1:4 ratio used in the NOE experiments (Brown and Huestis, 1993), rather than an artifact of the simulation. For example, in our recent simulations of the fusion-inhibiting peptides (Z-D-Phe-L-Phe-Gly) (Richardson et al., 1980; Richardson and Choppin, 1983; Yeagle et al., 1992) interacting with N-methyl dioleoylphosphatidylethanolamine bilayers, we have observed that the order parameters vary dramatically because of the perturbing effect of the peptides (Damodaran and Merz, 1995).

Peptide dynamics

Structural studies of the peptide in the bilayer bound state and in solution by NMR showed that while the peptide has no preferred structure in solution, it adopts a conformation in the bilayer with the Phe rings having close interaction with C_α of Ala-3 and the tert-butyl group (Brown and Huestis, 1993). We have examined the peptide dynamics by using RMS deviations of the peptide heavy atoms in solution and in the bilayer. The RMS deviations shown in Fig. 8 were calculated by aligning the Phe-2 and Ala-3 backbone

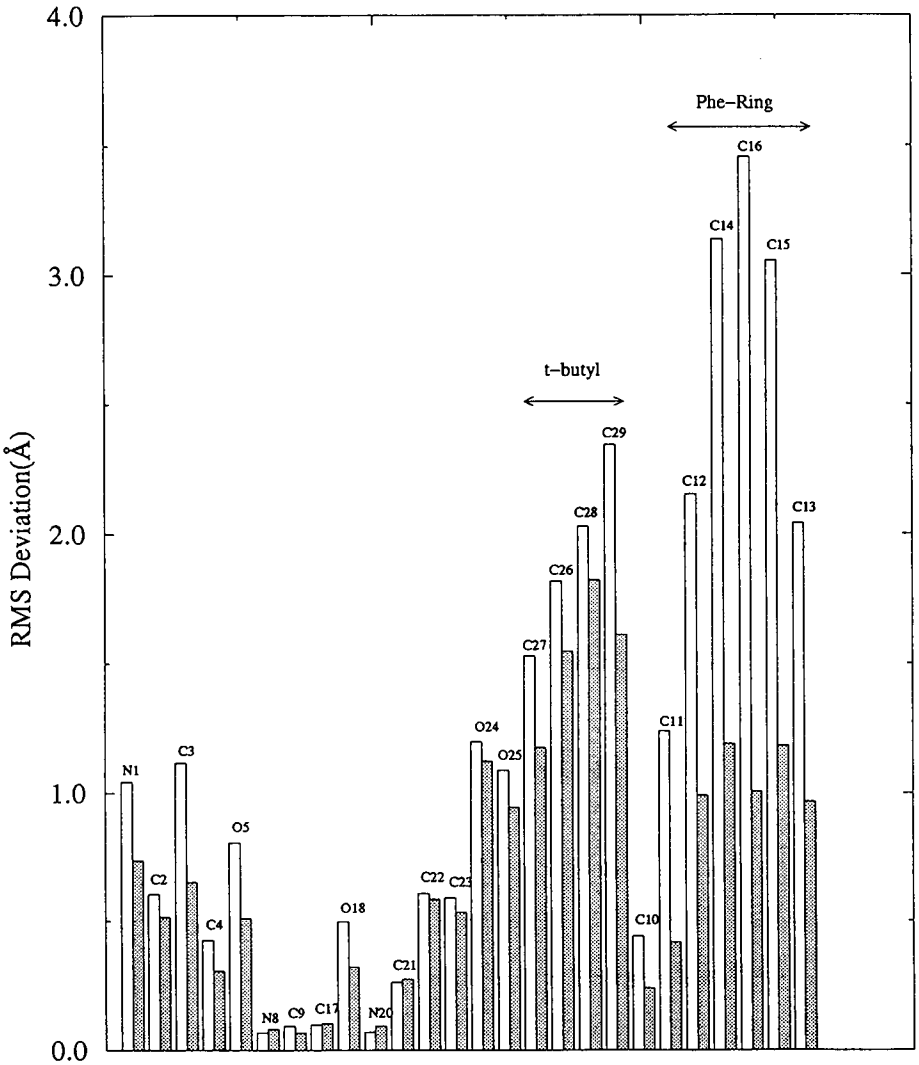

FIGURE 8 Calculated RMS deviations for the peptide heavy atoms in the bilayer (*shaded bars*) and solution (*unshaded bars*). The bilayer data were obtained as the average of both the peptides in the model. Data are for model II only.

atoms of a series of structures along the MD trajectory. As expected, the RMS deviations are larger in solution than in the bilayer. However, a more interesting aspect of Fig. 8 is the significant increase in the RMS deviations for the Phe ring (atoms C10-C13) in solution relative to other regions of the peptide, including the tert-butyl group (atoms C27-C29). Fig. 8 also suggests that the tert-butyl group has the largest mobility in the bilayer, whereas in solution the Phe ring has the highest motional freedom.

We have also monitored the time dependence of various proton-proton distances in the peptides in the bilayer along the MD trajectory by generating the positions of the protons attached to the carbon atoms with use of standard geometries. The starting structures for the peptides were generated by minimizing them subject to the NOE restraints. However, these structures relaxed somewhat during the equilibration phase, when no restraints were applied. This was particularly true in the case of peptide-2 where the tert-butyl group extended into the alkyl chain region, whereas the NMR structure places the tert-butyl group in proximity to the Phe 2 ring (Brown and Huestis, 1993). Consequently, the proton-proton distances satisfied the NOE criteria only during a fraction of the total MD trajectory. These differences could be due to the shorter time scales used in the MD simulations relative to the NMR timescale (10^{-6}-10^{-5} s vs. 10^{-12} s). Another reason for the observed differences could be the concentration effects. The NMR study employed a lipid/peptide ration of 4:1 (we used a ratio of 8:1 in the MD simulation), which could place adjacent peptides very close to one another. If the environment is "rigid" enough or if there is peptide aggregation, interlipid NOE contacts could be formed. It would be interesting to repeat the NMR experiments at several lipid/peptide ratios in order to determine whether concentration effects are present.

Lipid dynamics

We have studied the lipid dynamics by calculating the velocity autocorrelation functions ($c(t)$) for the head group atoms and the alkyl chain atoms, which were then compared with similar information obtained from a neat DMPC simulation (Damodaran and Merz, 1994). These velocity auto-

correlation functions and the corresponding spectral density functions (I(ω)) were obtained as equations 3 and 4, respectively.

$$c(t) = \frac{\langle v(0)v(t)\rangle}{\langle v(0)v(0)\rangle} \tag{3}$$

$$I(\omega) = \int_0^{t_{max}} c(t)\cos(\omega t)dt \tag{4}$$

These functions are given in Figs. 9 and 10. The spectral densities have contributions mainly from torsional motions and head group rotational motion. The velocity autocorrelation function and the spectral density function are similar to those of neat DMPC for both the head group and alkyl chain motions. Slight differences in the intensities in the spectral density function were observed; however, the data as a whole indicate that the presence of the peptide does not significantly perturb the overall lipid dynamics on the picosecond time scale. (The maximum time length for calculating the correlation functions was ~30 ps.) The lipid dynamics are thus consistent with the response of the order parameters. Because the alkyl chain dynamics sampled in the simulation involves primarily *trans*-gauche isomerization, which may not be affected significantly by the peptides, this behavior may be expected. In the case of lipid head group motion, the strongest peptide-lipid interactions are probably the hydrogen bonds with the phosphate groups, which are not highly mobile. Thus the behavior of the lipid dynamics probed in the simulation appears to be consistent with the model.

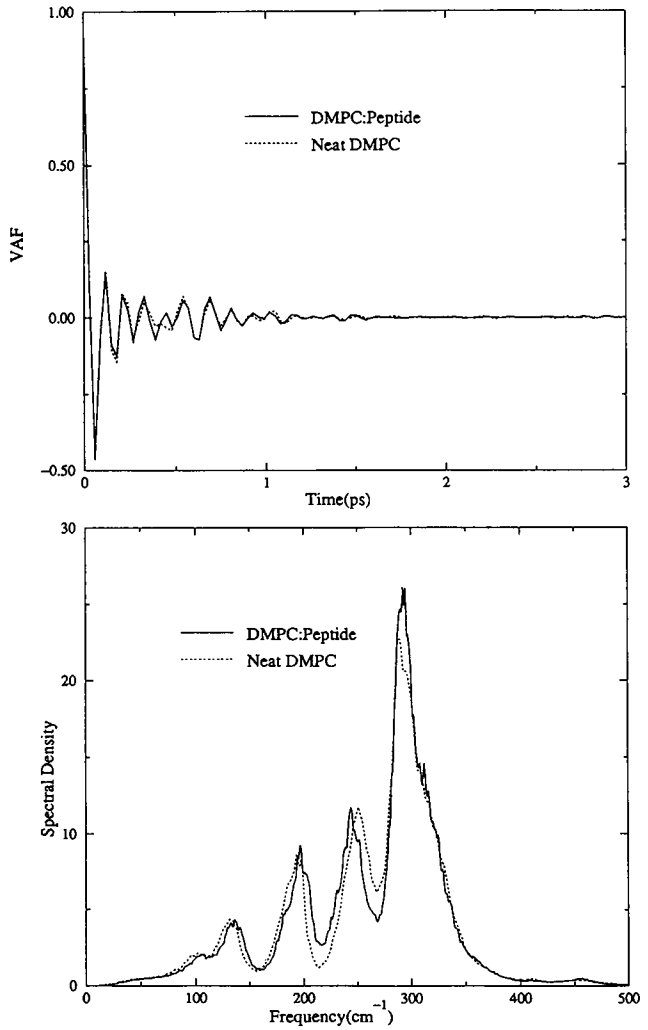

FIGURE 9 Velocity autocorrelation functions (*top*) and the corresponding normalized spectral density functions (*bottom*) for the lipid head groups for the leaflet with the peptides and neat DMPC. Data are for model II only.

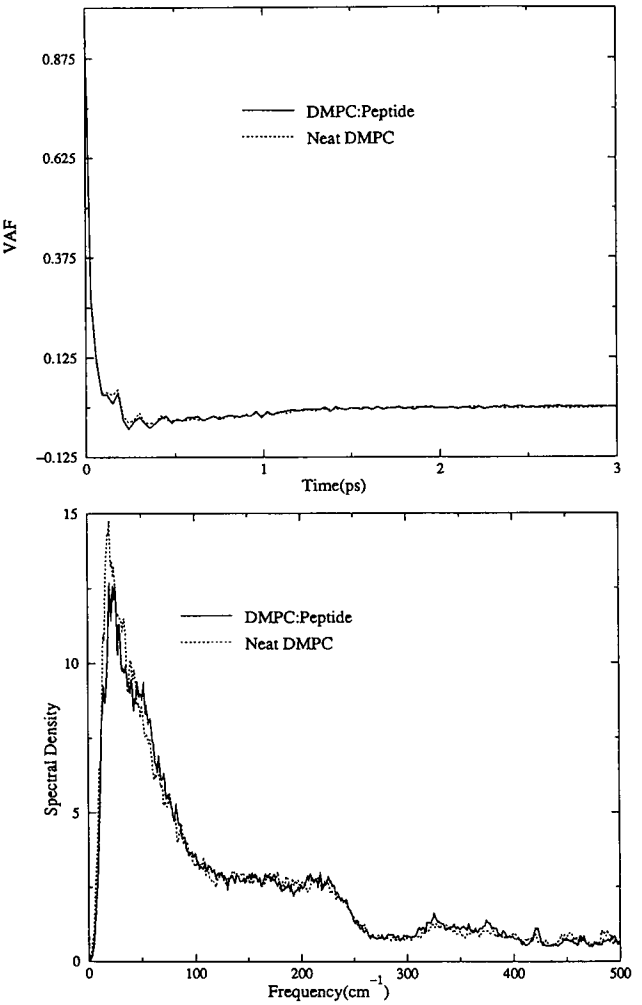

FIGURE 10 Velocity autocorrelation functions (*top*) and the corresponding normalized spectral density functions (*bottom*) for the alkyl chains for the leaflet with the peptides and neat DMPC. Data are for model II only.

CONCLUSIONS

Two 450-ps simulations of the lipid-peptide system (DMPC-AFAtBu) with explicit water molecules have been

carried out, and their structural and dynamical properties have been analyzed. In view of the extensive structural and thermodynamic data available for this system, it was considered a useful model system for investigating bilayer peptide interactions using molecular dynamics techniques. The peptides did not significantly affect the lipid dynamics or the average structure at the peptide/lipid ratios studied, although in model I a slight decrease in the order parameters was observed. The density profiles calculated from the simulation agreed well with the neutron diffraction data for the Ala-Trp-Ala-O-tert-butyl tripeptide on DOPC bilayers (Jacobs and White, 1989). Experimentally, as one goes down the Ala-X-Ala-O-tert-butyl (X = Trp, Phe, Leu, Ala, Gly) series of peptides, the free energy for partitioning of the peptides into the bilayer decreases from −5.12 kcal/ml for Trp to −2.91 kcal/ml for Gly (Jacobs and White, 1986). This difference is thought to be due to hydrophobic interactions between the lipid alkyl region and the central side chain. These peptides also have significant hydrogen bonding interactions between the peptide N-termini and the nonesterified oxygens of the lipid phosphate groups, which help to anchor them at the lipid-water interface (see Fig. 5 *a* and *b*).

Interesting insights have been obtained from the comparison of the dynamics of the peptides in solution and in the bilayer bound state. NMR data, which result from the average response of a large number peptides on a much longer time scale, suggest that the solution structure is essentially random, whereas the bilayer bound form adopts a preferred conformation wherein the Ala-3 C_α and the tert-butyl groups are closer to the Phe side chain. When we start with the NMR structure our simulations agree with this experimental observation, but we find that over the course of ~0.5 ns the peptides are not able to undergo substantial conformational changes. For example, in model I we began the simulations with an extended peptide backbone with the Phe intercalated into the bilayer and the tert-butyl group in the interfacial region. This overall conformation was then retained throughout the simulation. In model II, the tert-butyl group on peptide-2 is more extended into the bilayer whereas peptide-1 adopted a more compact geometry, adjacent to the Phe-2 side chain, and remained so throughout the simulation. Thus different peptides can adopt different conformations having lifetimes of several hundred picoseconds. This suggests that great care must be exercised when simulations with intercalated molecules are carried out. Many conformations should be tried and explored with long MD simulations before any quantitative conclusions are drawn. The use of an accurate starting geometry is also important in these simulations because the bilayer-water interface itself is a region of relatively low mobility, and the probability for any significant configurational rearrangement during the equilibration phase is rather limited. For example, we have observed this in the case for model I in which the tert-butyl group of the peptides were exposed to the aqueous region and could not be partitioned into the hydrocarbon region because of the low mobility of the head groups.

Finally, we find that the dynamics of the bilayer is not strongly affected by the presence of the peptide, which demonstrates the ability of the bilayer to accommodate molecules that perturb the lipid environment. This "plasticity" of the bilayer environment is not unexpected, given the weak interactions between the lipid constituents.

We thank the Office of Naval Research for supporting this research through Grant N00014-90-3-4002. The Pittsburgh Supercomputer Center and the Cornell Theory Center are acknowledged for generous allocations of parallel supercomputer time through a MetaCenter grant.

REFERENCES

Bassolino-Klimas, D., H. E. Alper, and T. R. Stouch. 1993. Solute diffusion in lipid bilayer membranes: an atomic level study by molecular dynamics simulation. *Biochemistry.* 32:12624–12637.

Berendsen, H. J. C., J. R. Grigera, and T. P. Straatsma. 1987. The missing term in effective pair potentials. *J. Phys. Chem.* 91:6269–6271.

Berendsen, H. J. C., J. P. M. Postma, W. F. van Gunsteren, A. D. DiNola, and J. R. Haak. 1984. Molecular dynamics with coupling to an external bath. *J. Chem. Phys.* 81:3684–3690.

Beschiaschvili, G., and J. Seelig. 1992. Peptide binding to lipid bilayers. Nonclassical hydrophobic effect and membrane-induced pK shifts. *Biochemistry.* 31:10044–10053.

Besler, B. H., K. M. J. Merz, and P. A. Kollman. 1990. Atomic charges derived from semiempirical methods. *J. Comput. Chem.* 11:431–439.

Brown, J. W., and W. H. Huestis. 1993. Structure and orientation of a bilayer-bound model tripeptide. A ^{1}H NMR study. *J. Phys. Chem.* 97:2967–2973.

Damodaran, K. V., and K. M. J. Merz. 1994. A comparison between DMPC and DLPE based lipid bilayers. *Biophys. J.* 66:1076–1087.

Damodaran, K. V., and K. M. J. Merz. 1995. Interaction of the fusion inhibiting peptide carbobenzoxy-D-Phe-L-Phe-Gly with N-methyldioleoylphosphatidylethanolamine lipid bilayers. *J. Am. Chem. Soc.* 117: 6561–6571.

Gennis, R. B. 1989. Biomembranes: Molecular Structure and Function. Springer-Verlag, New York.

Jacobs, R. E., and S. H. White. 1986. Mixtures of a series of homologous hydrophobic peptides with lipid bilayers: a simple model system for examining the protein-lipid interface. *Biochemistry.* 25:2605–2612.

Jacobs, R. E., and S. H. White. 1987. Lipid bilayer perturbations induced by simple hydrophobic peptides. *Biochemistry.* 26:6127–6134.

Jacobs, R. E., and S. H. White. 1989. The nature of the hydrophobic binding of small peptides at the bilayer interface: implications for the insertion of transbilayer helices. *Biochemistry.* 28:3421–3437.

Jorgensen, W. L., and J. Tirado-Rives. 1988. The OPLS potential functions for proteins: energy minimizations for crystals of cyclic peptides and crambin. *J. Am. Chem. Soc.* 110:1657–1666.

Lewis, B. A., and D. M. Engelman. 1983. Lipid bilayer thickness varies linearly with acyl chain length in fluid phosphatidylcholine vesicles. *J. Mol. Biol.* 166:211–217.

Merz, K. M., Jr. 1992. Analysis of a large database of electrostatic potential derived atomic point charges. *J. Comput. Chem.* 13:749–767.

Pearlman, D. A., D. A. Case, J. C. Caldwell, G. L. Seibel, U. C. Singh, P. Weiner, and P. A. Kollman. 1991. AMBER 4.0. University of California, San Francisco.

Richardson, C. D., and P. W. Choppin. 1983. Oligopeptides that specifically inhibit membrane fusion by Paramyxoviruses: studies on the site of action. *Virology.* 131:518–532.

Richardson, C. D., A. Scheid, and P. W. Choppin. 1980. Specific inhibition of paramyxovirus and myxovirus replication by oligopeptides with

amino acid sequences similar to those at the N-termini of the F_1 or HA_2 viral polypeptides. *Virology.* 105:205–222.

Seelig, A., and J. Seelig. 1974. The dynamic structure of fatty acyl chains in a phospholipid bilayer measured by deuterium magnetic resonance. *Biochemistry.* 13:4839–4845.

Seelig, J., and J. L. Browning. 1978. General features of phospholipid conformation in membranes. *FEBS Lett.* 92:41–44.

Seelig, J., and P. Ganz. 1991. Nonclassical hydrophobic effect in membrane binding equilibria. *Biochemistry.* 30:9354–9359.

Tanford, C. 1980. The Hydrophobic Effect: Formation of Micelles and Biological Membranes. John Wiley & Sons, New York.

Vincent, J. J., and K. M. Merz, Jr. 1995. A highly portable parallel implementation of AMBER 4 using the message passing interface standard. *J. Comput. Chem.* In press.

Weiner, S. J., P. A. Kollman, D. A. Case, U. C. Singh, C. Ghio, G. Alagona, S. Profeta, and P. Weiner. 1984. A new force field for molecular mechanical simulation of nucleic acids and proteins. *J. Am. Chem. Soc.* 106:765–784.

Yeagle, P. L., J. Young, S. W. Hui, and R. M. Epand. 1992. On the mechanism of inhibition of viral and vesicle membrane fusion by carbobenzoxy-D-phenylalanyl-L-phenylalanylglycine. *Biochemistry.* 31: 3177–3183.